ACS APPLIED MATERIALS & INTERFACES

Research Article

www.acsami.org

Degradation and Healing Mechanisms of Carbon Fibers during the Catalytic Growth of Carbon Nanotubes on Their Surfaces

Kyoung Ju Kim,[†] Woong-Ryeol Yu,*[,†] Ji Ho Youk,[‡] and Jinyong Lee[§]

[†]Department of Materials Science and Engineering, Seoul National University, Seoul 151-742, Korea

[‡]Department of Advanced Fiber Engineering, Inha University, Incheon 402-751, Korea

[§]High Temperature Composite Materials Group, Agency for Defense Development, Daejeon 305-600, Korea

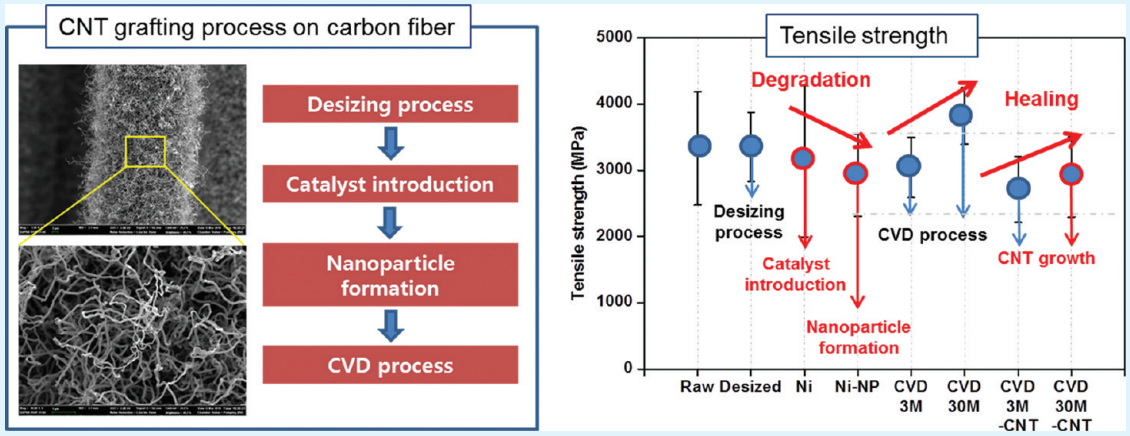

ABSTRACT: This study reports on the main cause of the reduced tensile strength of carbon fibers (CFs) by investigating the microstructural changes in the CFs that are undergoing mainly two processes: catalyst nanoparticle formation and chemical vapor deposition (CVD). Interestingly, the two processes oppositely influenced the tensile strength of the CFs: the former negatively and the latter positively. The catalysts coating and nanoparticle formation degraded the CF surface by inducing amorphous carbons and severing graphitic layers, while those defects were healed by both the injected carbons and interfaced CNTs during the CVD process. The revealed degradation and healing mechanisms can serve as a fundamental engineering basis for exploring optimized processes in the manufacturing of hierarchical reinforcements without sacrificing the tensile strength of the substrate CFs.

KEYWORDS: *hierarchical reinforcement, catalytic growth, carbon nanotube, carbon fibers, tensile strength, degradation and healing*

1. INTRODUCTION

Because of their stiffness, strength, and lightness, carbon fibers (CFs) have been widely used for advanced structural composites in various areas such as airplanes, satellites, and sporting goods.[1] Several factors determine the performance of CF-reinforced composites, including the mechanical properties of the individual CFs, the matrix properties, the fiber-matrix interface, and processing conditions.[2] Since the load in the composites is transferred from the matrix to the fiber through the shear stress, the control of the fiber-matrix interface is effective in ensuring good interfacial shear strength (IFSS) and, thus, improving the mechanical properties of the CF-reinforced composites.

Recently, the direct growth of carbon nanotubes (CNTs) onto CF surfaces has been newly proposed to modify the fiber-matrix interface and, thus, increases the IFSS[3] since the nanoscale CNTs increase the surface area, create mechanical interlocking, and/or induce local stiffening at the fiber-matrix interface all of which can improve the stress transfer and interfacial properties.[4] In addition, CNTs grown on conventional fiber surfaces increase the loading of the CNTs in the radial orientation, which may be optimal for transverse reinforcement.[5] The potential benefits of these nanoscale CNTs combined with micrometer-scale CFs have promoted extensive research toward developing multiscale hybrid composites with tailored physical properties.[6]

CNTs have been directly grown on CF surfaces using chemical vapor deposition (CVD).[3−15] The catalytic growth of CNTs strongly depends on process conditions such as the CVD temperature,[8] various carbon sources[9] and their flow rates,[10,12] and the type and concentration of the catalyst.[3] These conditions influence the mechanical properties of the CNT-grafted-CFs and their composites,[4−7] but unanimously, the interfacial properties of the composites were reported to be enhanced by grafting the CNTs on the CF surfaces. Most of these studies, however, reported a reduction in the tensile

Received: February 13, 2012
Accepted: April 5, 2012
Published: April 5, 2012

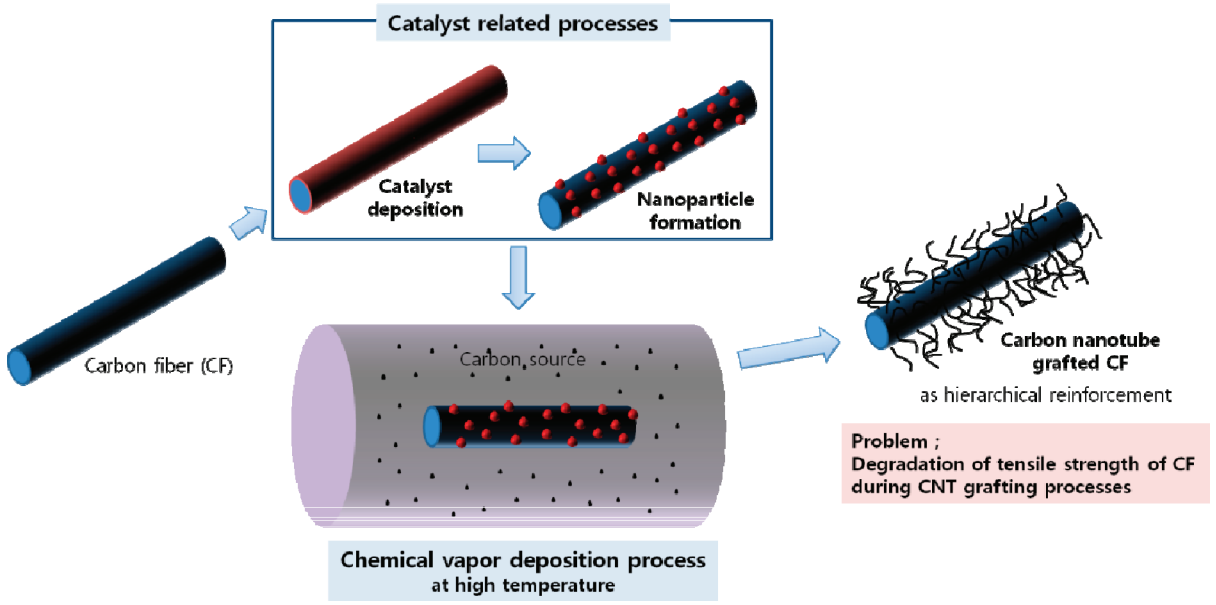

Figure 1. Schematic diagram of the catalytic growth of CNTs on the CF surfaces.

strength of the CFs as much as 10−50%[4,5,7,15] except one paper.[14] Such degraded properties of the CFs were explained just by possible surface flaws on the CF through thermal degradation and surface oxidation during the CVD process[7] or possible internal damages caused by the harsh environment of the CVD process.[16] The main reason for the reduced tensile strength is not clear yet; however, it must be a severe obstacle for the successful progression of the hierarchical modification method (nanoscale CNT growth on the micrometer-scale CF surface).

In this study, we traced the microstructural changes and the tensile strength of CFs during the entire process of catalytic growth for CNTs with the following steps: desizing the CFs, coating the catalyst film, forming the catalytic nanoparticles, and growing the CNTs through the CVD process (see Figure 1). The effect of each step in the process on the CFs was quantified to determine which process was responsible for the reduced tensile strength of the CFs. In the remainder of the paper, the mechanisms for such reduced tensile strength are revealed, which can be a basis for exploring optimized processes in the manufacturing of nanoscale CNTs grown on micrometer-scale CFs without sacrificing the tensile strength of the CFs.

2. EXPERIMENTAL SECTION

2.1. Materials. High strength CFs (T700SC-12000-50C, Toray) with sizing agents were cleaned in distilled water by ultrasonic vibration for 30 min and then used as the substrate for the growth of CNTs. The sizing agents on the CF surfaces were removed with heat treatment since they may interact with subsequent processes such as the CVD and the introduction of the catalysts processes. Heat treatment was done at 400 °C for 2 h.

2.2. Catalytic Growth of CNTs on CFs. *2.2.1. Prior Process: Catalyst Nanoparticle Formation.* A nickel (Ni) catalyst thin film was coated on the desized CF surfaces using a sputtering method. The aligned CFs that were in a frame were put into the sputter. Sputtering was then carried out twice for the uniform deposition of Ni atoms onto the CF surfaces: one side was deposited and then the frame was turned upside down so that the other side could undergo sputtering. The sputtering process was done with an Ar gas flow rate of 40 sccm using a metal sputter (MHS-1500). The catalyst deposition on the CFs was confirmed with energy dispersive X-ray spectroscopy (EDS). The thickness of the coated Ni film was controlled to be 22 nm. The Ni film was then annealed for 5 min raising the temperature from 700 to 750 °C using hydrogen and argon gases with a feeding rate of hydrogen/argon = 50 sccm:450 sccm. The morphologies of the formed nanoparticles were observed with field emission-scanning electron microscopy (FE-SEM, SUPRA 55VP from Carl Zeiss, Inc.).

2.2.2. Main Process: CVD. CNTs were synthesized on the CF surfaces by the CVD process using a tubular furnace. The CNTs were grown at 750 °C with a carbon source (C_2H_2) in the carrier gases (Ar and H_2). The feeding rate of these gases was set to be 50, 50, and 450 sccm for acetylene, hydrogen, and argon, respectively. The CVD time (3 and 30 min) were varied to investigate the effect of the CVD characteristics on the CF mechanical properties and growth of the CNTs. Note that hydrogen gas was not injected for 3 min CVD because CNT was grown well for a short time CVD without hydrogen gas. The CVD process was carried out again to desized CFs but without a catalyst present. This experiment was done to investigate the effect of the CVD environment itself on the CF strength by excluding any interaction between the catalytic nanoparticles and the CF surfaces.

2.3. Mechanical and Microstructural Characterizations. After each process (Ni catalyst coating, Ni nanoparticle formation, and catalytic growth of CNTs), individual CFs were collected and characterized. The tensile strength was measured using the single-fiber tensile testing method in accordance with ASTM D3822-07. A single fiber was carefully separated from the CF bundles and attached to a paper tab using adhesive. The gage length of the fiber was 20 mm, and the extension rate was set to 2 mm/min. The single-fiber tensile test was conducted for at least 20 single fibers using a microload tensile tester with a load sensor of 100 g.

The microstructures of the CFs were investigated with high-resolution-transmission electron microscopy (HR-TEM, JEM-3000F from JEOL Ltd.). TEM specimens were prepared using ultramicrotome (RMC MTX from Boeckler Instruments) with a diamond knife and focused ion beam (FIB) (SMI3050SE from SII Nanotechnology Inc.) technique. To observe CNTs grown on CFs, a CNT grafted CF was mounted using epoxy resin in a mold. After curing the epoxy, the molded block was separated from the mold. Several thin films were obtained by slicing the block using an ultramicrotome and were positioned on the TEM grid. To observe the surface of carbon fibers, FIB was used. First, the carbon fibers were fixed on a silicon

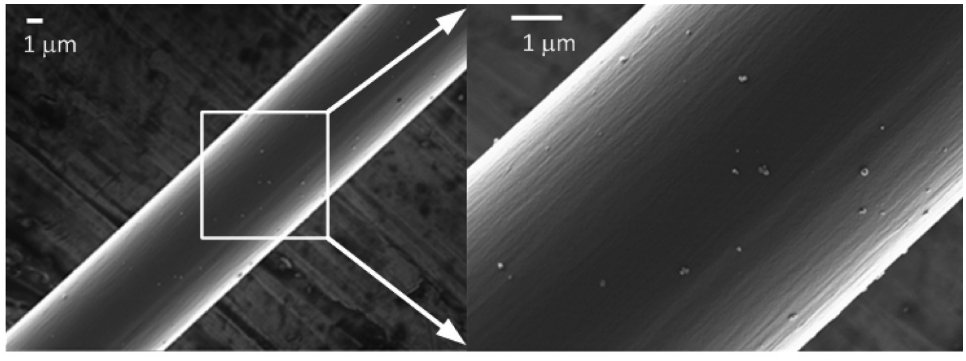

(a)

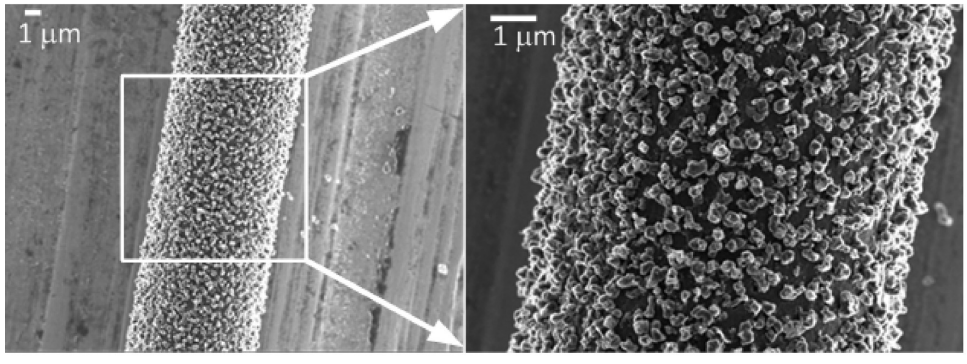

(b)

Figure 2. Morphologies of the CF surfaces (a) after catalyst coating and (b) after subsequent nanoparticle formation.

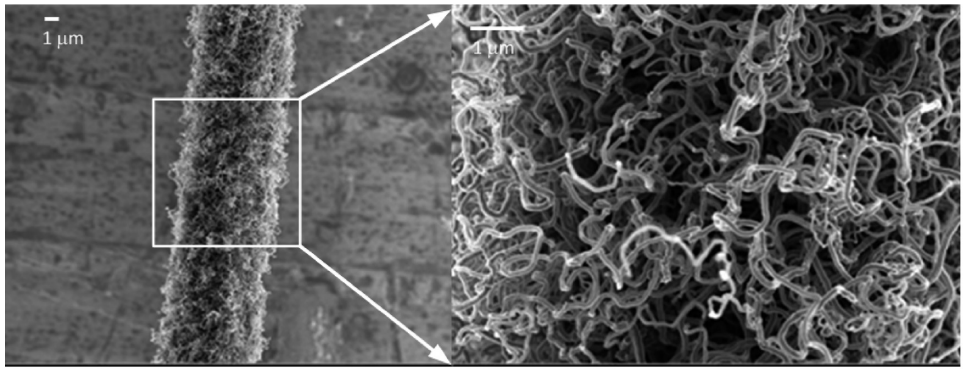

(a)

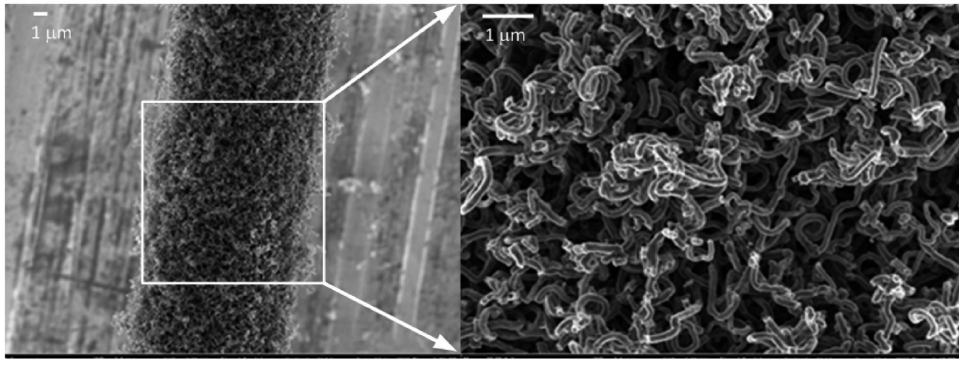

(b)

Figure 3. Morphologies of the CNTs grown on the CFs according to the CVD process time: (a) 3 and (b) 30 min.

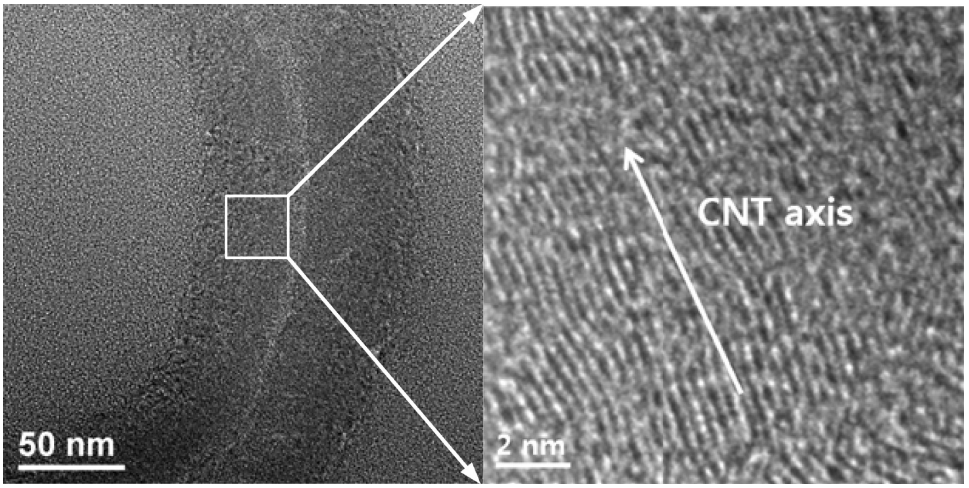

Figure 4. TEM images of CNTs grown on the CF surfaces.

wafer. The amorphous carbons were then deposited on the surface of the carbon fiber to prevent the damage during the FIB process. The Ga^+ ions in FIB were then used, and their intensity was controlled for shaping and finishing the cross sections of the sample.

Since the microstructural changes in the CFs are closely related to their mechanical properties,[17,18] wide-angle X-ray diffraction (WAXD, D8-Advance diffractometer from Bruker Miller Co.) analysis was done for a scanning range from 5° to 80° at a scan rate of 4.22° min^{-1}. The wavelength of the beam was 0.154 06 nm (Cu Kα1 line). Raman spectra were also obtained with a Raman spectrometer (T64000 from Horiaba Jobin Yvon) and with the green line of an argon laser using a wavelength of 514 nm. The Raman spectra of carbonaceous materials have two characteristic bands: the D-band and G-band, which are centered at wavenumbers of ~1350 and ~1600 cm^{-1} and are related to disordered carbonaceous structures and ordered graphitic structures, respectively. The intensity ratio of the two bands (I_D/I_G) indicates the amount of structurally ordered graphite crystallites in the carbonaceous materials.[19−22] The ratio of the I_D/I_G was obtained from static scans of the Raman spectra using a Lorentzian curve-fitting procedure for the D- and G-bands. For this, the D- and G-bands were separated using a software (OriginPro 8) after the straight baseline was drawn for background.

3. RESULTS AND DISCUSSION

3.1. Variations in the Tensile Strength of the CFs. First, the morphologies of the CFs were checked to confirm that the processes used in this study were indeed suitable for growing CNTs on CF surfaces. Ni nanoparticles are the starting point for the catalytic growth of CNTs. Figure 2 shows the Ni nanoparticles were successfully converted from the Ni thin film. The Ni film is not seemingly observable in Figure 2a, but it was confirmed by our EDS study. The nanoparticles in Figure 2b were uniformly formed, implying that the thermal treatment conditions with hydrogen gas were optimal. The morphologies of CNTs grown on the CF surface are shown in Figure 3. The CNTs were not straight but curled and entangled with each other, which can be explained by the nanoparticles scattered on the CF surfaces. Densely packed catalytic nanoparticles allow aligned and straight CNTs to be grown on a SiO_2/Si or Al_2O_3 substrate, in particular under plasma CVD;[23−25] however, entangled CNTs are more beneficial in terms of IFSS due to the increased surface area with the matrix interface.[7] On the other hand, a longer CVD time yielded longer and thicker CNTs as reported elsewhere.[26] Next, the microstructure of the CNTs was observed with HR-TEM to check whether they had a tubular structure wrapped with graphitic layers. Figure 4 shows the vacant hollow and graphene layers, concluding that the sequential processes used in this study was suitable for catalytically growing CNTs on CF surfaces.

The variation in the CF tensile strength during the grafting process was investigated using the single-fiber tensile test (Figure 5). The results yielded three interesting points. First,

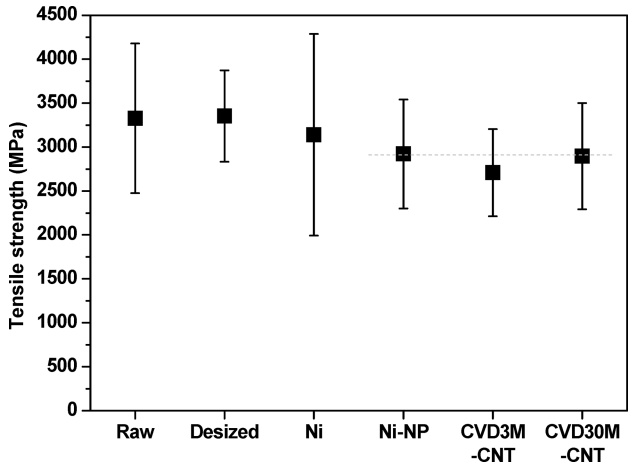

Figure 5. Variations in the tensile strength of the CFs for the sequential processes of the catalytic growth of CNTs. The tick labels Ni, Ni-NP, and CVD-CNT represent Ni catalyst coating, Ni nanoparticle formation, and catalytic growth of CNTs, respectively, and "3M" and "30M" mean a CVD process time of 3 and 30 min, respectively.

the tensile strength of the CF was maintained during the desizing treatment. It is not surprising since from the preliminary study, the treatment temperature and time were actually chosen not to induce any structural changes in the CFs but to burn out the sizing agent. Second, the tensile strength of the CFs was slightly reduced by the catalyst coating (sputtering). The situation became worse after the nanoparticle formation process. After the two prior processes (coating and thermal treatment), the tensile strength was reduced by as much as 11%, clearly indicating that the degradation on the CF surfaces occurred during these processes. Third, the main process (CVD) did not incur any further damages on the CF surfaces; and furthermore, it healed the damaged structure. The short duration of the CVD process resulted in a slight reduction

in the tensile strength of the CFs; however, an increased CVD time attenuated the reduction, implying that the damages before the CVD process can be healed. This possibility of healing is an important finding that offers an opportunity to optimize the sequential processes for the catalytic growth of CNTs on surfaces without sacrificing the tensile strength of the CFs. For this to occur, the degradation and healing mechanisms in the prior processes and main process need to be revealed.

3.2. Degradation Mechanism of the CFs in the Coating and Annealing Processes. Two possibilities could explain such degradation of the CF strength during the coating and annealing processes: changes as well as damages in the crystal structure. X-ray diffraction (XRD) analysis was carried out to investigate whether any structural changes in the carbon crystals occurred during the catalyst coating and annealing processes. The main peak was observed at approximately 26.2° (2θ) (see Figure 6), corresponding to

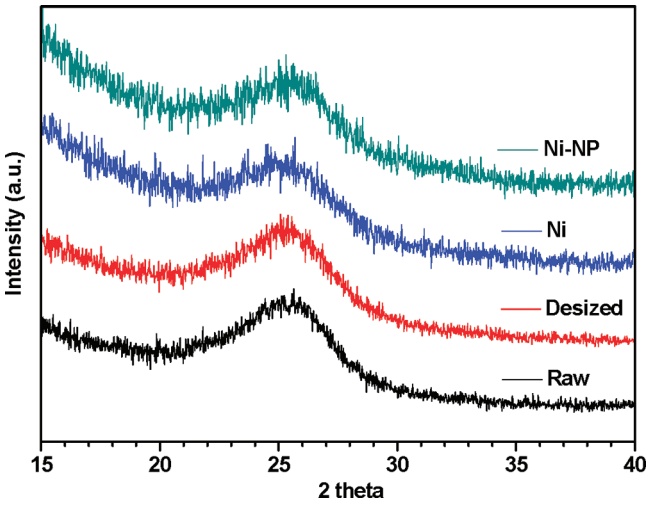

Figure 6. XRD analysis of the CFs after the individual prior processes (coating and annealing) for the catalytic growth of CNTs. The label Ni and Ni-NP represent Ni catalyst coating and Ni nanoparticle formation, respectively.

the (002) reflections of the pseudographitic structure.[27,28] The interplanar spacing of the graphitic layers in the CFs was calculated and was not affected by the catalyst related processes, meaning that the crystal structure did not change. The broadening of the main peak, however, was observed probably due to the deteriorated crystal quality. Next, the I_D/I_G ratio in the Raman spectrum was traced to check for possible damage on the CF surfaces.[29] Figure 7 shows variations in the I_D/I_G ratio according to the sequential processes taking place (refer to Table 1 for actual values). A negligible change was observed after the desizing process. The ratio increased slightly after the catalyst coating and then further increased significantly after the annealing for nanoparticle formation. Damages or changes in the graphitic layers of the CFs clearly occurred, which were revealed by TEM observation.

The TEM image of a desized CF is presented in Figure 8a, showing the turbostratic carbon crystals preferably oriented along the fiber axis. After the Ni catalyst coating, the CF surfaces were dramatically changed shown in Figure 8b. The Ni layer was clearly on top of the CF surfaces (see "Region I" in Figure 8b). Below it, the amorphous carbon layers were observed with very small catalytic nanoparticles in "Region II",

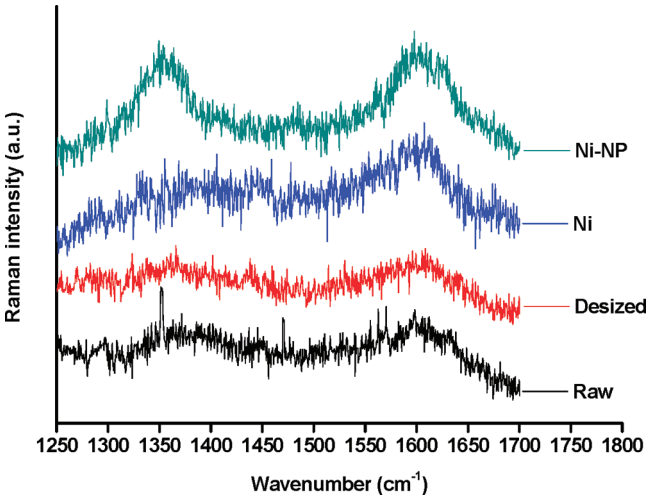

Figure 7. Raman spectrum of the CFs after the individual prior processes (coating and annealing) for the catalytic growth of CNTs. The label Ni and Ni-NP represent Ni catalyst coating and Ni nanoparticle formation, respectively.

Table 1. I_D/I_G of the CFs Determined from the Raman Spectra

	I_D/I_G	process explanation
raw	0.80	none
desized	0.78	desizing
Ni	0.87	Ni film
Ni-NP	0.99	Ni nanoparticle
Anneal3M	0.82	annealing without carbon source and catalysts
CVD3M	0.80	CVD (3 min) with carbon source and without catalysts
CVD30M	0.59	CVD (30 min) with carbon source and without catalysts

which can be deduced as Ni_3C from the literature.[30,31] The amorphous layer was formed by the Ni atoms diffused from the outer layer of the CF surfaces and spanned up to about 26 nm in depth. This damages decrease the load carrying capability of CFs, as observed in Figure 5.

Next, the microstructure of the CFs was observed after the annealing, which sequentially followed the Ni catalyst coating process. Figure 9 shows that Ni nanoparticles had formed on the surfaces of the CFs. Interestingly, the nanoparticles were located below the CF surfaces, alluding to the fact that the Ni atoms were diffused into the CF surfaces, leaving many grooves on the CF surfaces (see the white arrows in Figure 9). Such nanoparticles severed many graphitic layers of the CFs and dug into the CFs up to 78 nm in depth (see the right picture in Figure 9). In this case, the area of the damage was approximately calculated to be 4.5% of the cross-sectional area of the CFs using the penetration depth (78 nm) and the diameter of the CF (7 μm). The reduction in the tensile strength, however, was as much as about 11%, which is greater than the damaged portion. This can be explained by the core-skin structure of the PAN-based CFs. The skin layers in PAN-based CFs tend to have more carbon layers lined up parallel to the fiber perimeter than the core part exhibiting a random cross-sectional texture (also called the turbostratic texture).[32] This structural characteristic is the main reason why defects formed on CF surfaces are fatal to the tensile strength of the CFs as observed above.

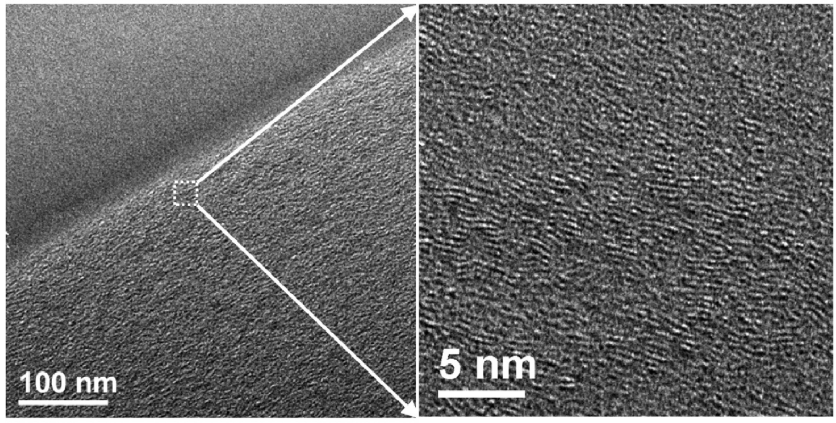

(a)

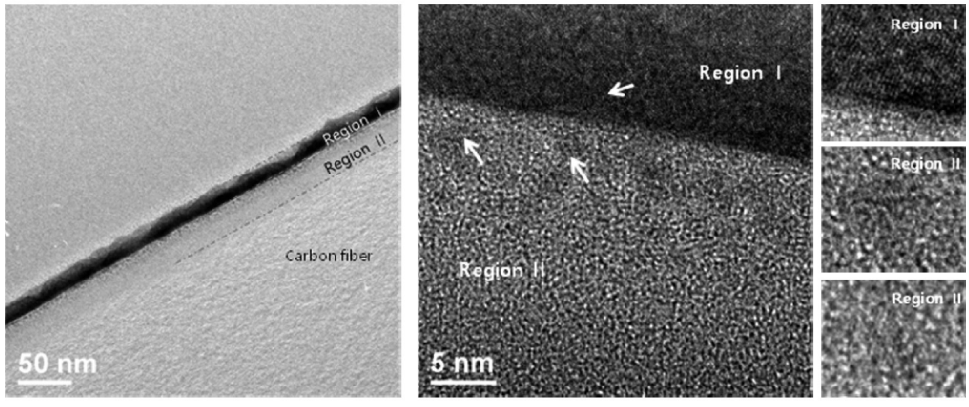

(b)

Figure 8. TEM images of the CF surfaces (a) and (b) after catalyst coating. Note that Regions I and II represent the Ni film and beneath it on the carbon fiber surface, respectively.

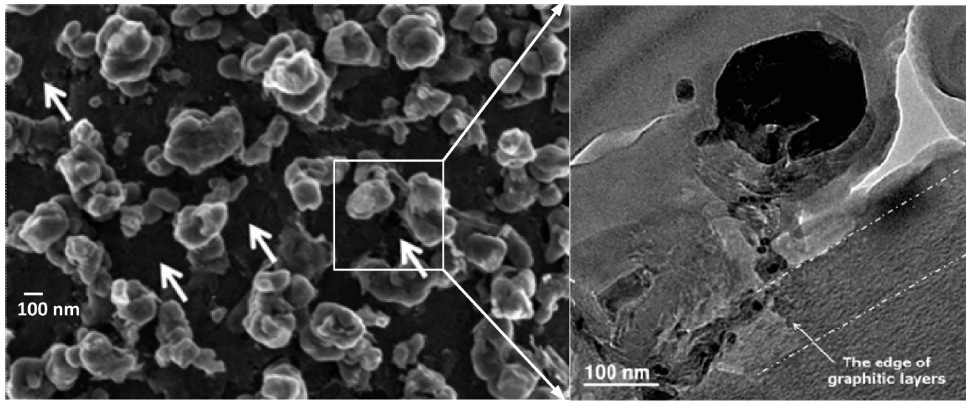

(a) (b)

Figure 9. Morphologies of the CF surfaces and Ni nanoparticles: (a) FE-SEM image and (b) HR-TEM image.

3.3. Healing Mechanism during the Main Process (CVD). The subsequent process after the catalyst coating and annealing is to catalytically grow CNTs by the CVD process, in which a carbon source is provided at high temperature. It would not be unusual to assert that such reactive conditions at high temperature during the CVD process is another source of defects in the substrate CFs; however, in truth, this is a controversial issue. It has been reported that CFs can be degraded due to surface flaws generated through the CVD process,[7] whereas the mechanical properties of the CFs can be improved at high temperature and inert environments.[15] Here, we investigated which effects were dominant during the CVD process. First, we wanted to exclude the catalytic effects by performing the CVD process on desized CFs under the same conditions previously used for the growth of CNTs except without any coated catalysts.

The variations in the tensile strength of the CFs were measured again after the CVD process without catalysts. In other words, we define "without catalysts" to mean that no CNTs were grown after the CVD process. Figure 10 shows that

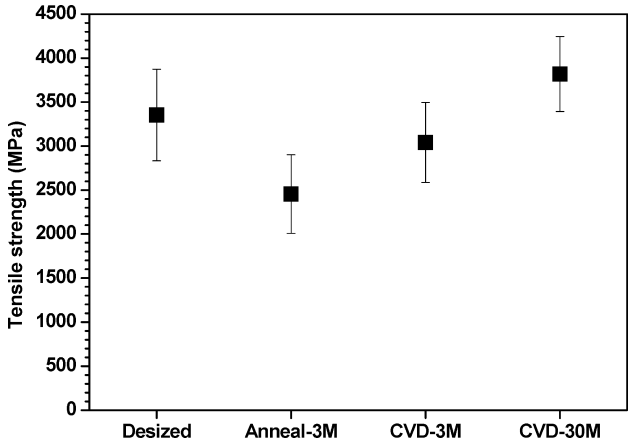

Figure 10. Tensile strength of the CFs undergoing the annealing and the CVD process without any catalyst. The tick label "Anneal" denotes just the thermal treatment at 750 °C without a carbon source, whereas "CVD" denotes the thermal treatment at 750 °C with a carbon source. The numbers in the tick label are the treatment time.

the reduced tensile strength was due to thermal treatment at 750 °C for 3 min. The effect of the carbon source was observed when it was provided to the CFs at the same temperature as the thermal treatment case above. The carbon source also brought about a reduction in the tensile strength of the CFs; however, the actual degree to which the tensile strength was reduced was smaller than that of the thermal case without a carbon source, implying that the carbon source had a role in reducing the damage on the CF surfaces. When the CVD time increased, surprisingly, the tensile strength of the CFs increased to even larger values than that of both the as-received and desized CFs. Therefore, the findings suggest that the carbon source provided for the CVD process helped in recovering the damages on the CF surfaces, i.e., a healing effect occurs during the CVD process. To investigate the mechanisms behind these results, XRD and Raman analyses were carried out again.

It is well-known that a graphite structure can be stabilized by a high temperature annealing process.[33,34] In this study, the XRD peaks and the interplanar spacing ("d_{002}") were not affected by the annealing shown in Figure 11 since the annealing temperature was not so high to cause turbostratic structures. However, a change in the Raman spectrum was observed (see Figure 12), showing broadened peaks, which was probably due to the appearance of another defect related to amorphization, which might be caused from the turbulence of the basal planes.[33] The I_D/I_G ratio in Table 1 increased, providing a decisive clue to the reduced tensile strength caused by the annealing. The high-temperature annealing adopted in this study brought about the disorder in the graphite layers, i.e., turbulence in the basal layers on the carbon fibers.

The carbon source provided in the annealing did not influence the crystal structure of the CF fibers as in the "without carbon source" case. The I_D/I_G ratio, however, was reduced, suggesting that the carbon source prevented or healed the disorder in the graphites of the CFs seen in the pure annealing case. A longer injection of the carbon source dramatically reduced the I_D/I_G ratio, strongly suggesting that

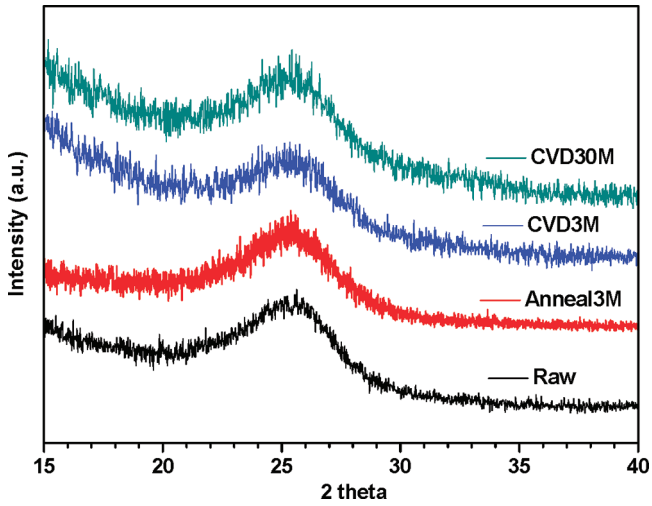

Figure 11. XRD analysis of the CFs undergoing the annealing and the CVD process without catalysts. The label "Anneal" denotes just the thermal treatment at 750 °C without a carbon source, whereas "CVD" denotes the thermal treatment at 750 °C with a carbon source. The numbers are the treatment time.

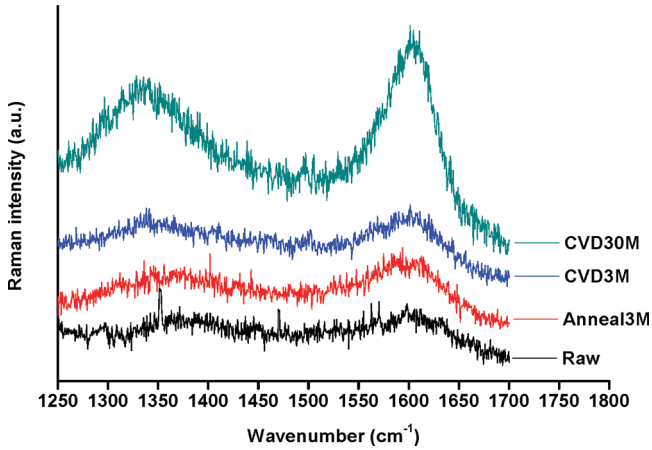

Figure 12. Raman spectrum of the CFs undergoing the annealing and the CVD process without catalysts. The label "Anneal" denotes just the thermal treatment at 750 °C without a carbon source, whereas "CVD" denotes the thermal treatment at 750 °C with a carbon source. The numbers are the treatment time.

the disorders in the graphite structures were healed with the help of the injected carbons; for example, they may have bridged the edges of the graphitic with high energy. It also can accompany the annealing effect for a long CVD process time since the defects that formed for the short annealing time easily disappeared upon annealing.[33] This healing and annealing resulted in the sharp peak at the G-band in the Raman spectra (see the "CVD30M" case in Figure 12). The CF surface was observed using HR-TEM to investigate the microstructural change in CF during the CVD process. There is no significant change inside CFs after CVD; however, new and dense graphitic layers were formed on the CF surface (see the "A" region in Figure 13). These graphitic layers indicate that the defects incurred during the previous process can disappear and another graphitic layers can be formed in the defect area (like a groove), healing the CF surface.

As a result, it can be claimed that the carbons provided in the CVD process are definitely the source of the CNTs grown on

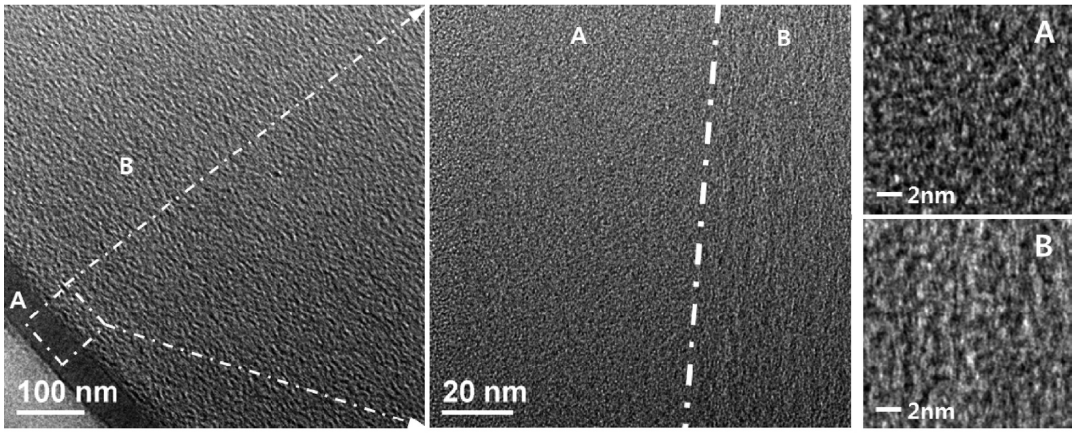

Figure 13. The microstructure of the CF surface after the CVD process without catalysts (CVD30M). Regions A and B are newly formed (and dense) graphitic layers and original graphitic on the CF surface, respectively.

the CF surfaces and, furthermore, can be a source of healing the graphite structure, which was damaged during the prior processes before the CVD process. Since the CFs used in section 3.3 have no catalytic nanoparticles, the claim above is not directly projected to CFs with catalytic nanoparticles; however, it is concrete enough to explain the maintained tensile strength of the CFs after the CVD process for the growth of CNTs in Figure 5.

4. CONCLUSIONS

The aim of this paper was to pursue concrete explanations for the variations in the tensile strength of the CFs undergoing the catalytic growth of CNTs on their surfaces. It was revealed that catalyst coating and nanoparticle formation were the main processes responsible for the reduced tensile strength in the CFs, whereas the CVD process itself did not cause any damages in the CFs but instead healed them if the proper CVD process time was maintained. The catalyst coating generated an amorphous region below the CF surfaces and the catalytic nanoparticles dug into, i.e. penetrated, the graphite layers, both of which induced defects in the CFs and caused the reduced tensile strength of the CFs. In contrast, carbon sources provided during the CVD process healed the damages probably by bridging the damaged edges of the graphite layers. These findings offer an opportunity to find the optimized processes to catalytically grow CNTs without sacrificing the tensile strength of the CFs, for example, minimizing the thickness of the coated catalyst, and prolonging the CVD process time within a cost-effective range.

AUTHOR INFORMATION

Corresponding Author

*Phone: +82 2 880 9096. Fax: +82 2 883 8197. E-mail: woongryu@snu.ac.kr.

Notes

The authors declare no competing financial interest.

ACKNOWLEDGMENTS

This work was supported by DAPA and ADD and by a Korea Science and Engineering Foundation (KOSEF) grant funded by the Korean government (MEST) (Grant R11-2005-065) through the Intelligent Textile System Research Center (ITRC).

REFERENCES

(1) Chae, H. G.; Kumar, S. *Science* **2008**, *319*, 908−909.
(2) Dhakate, S. R.; Bahl, O. P. *Carbon* **2003**, *41*, 1193−1203.
(3) Zhao, J. O.; Liu, L.; Guo, Q. G.; Shi, J. L.; Zhai, G. T.; Song, J. R.; Liu, Z. J. *Carbon* **2008**, *46*, 380−383.
(4) Qian, H.; Bismarck, A.; Greenhalgh, E. S.; Shaffer, M. S. P. *Compos. Sci. Technol.* **2010**, *70*, 393−399.
(5) Qian, H.; Bismarck, A.; Greenhalgh, E. S.; Kalinka, G.; Shaffer, M. S. P. *Chem. Mater.* **2008**, *20*, 1862−1869.
(6) Thostenson, E. T.; Li, W. Z.; Wang, D. Z.; Ren, Z. F.; Chou, T. W. *J. Appl. Phys.* **2002**, *91*, 6034−6037.
(7) Sager, R. J.; Klein, P. J.; Lagoudas, D. C.; Zhang, Q.; Liu, J.; Dai, L.; Baur, J. W. *Compos. Sci. Technol.* **2009**, *69*, 898−904.
(8) Zhu, S.; Su, C.-H.; Lehoczky, S. L.; Muntele, I.; Ila, D. *Diamond Relat. Mater.* **2003**, *12*, 1825−1828.
(9) Otsuka, K.; Abe, Y.; Kanai, N.; Kobayashi, Y.; Takenaka, S.; Tanabe, E. *Carbon* **2004**, *42*, 727−736.
(10) Zhao, Z.-G.; Ci, L.-J.; Cheng, H.-M.; Bai, J.-B. *Carbon* **2005**, *43*, 663−665.
(11) Riccardis, M. F. D.; Carbone, D.; Makris, T. D.; Giorgi, R.; Lisi, N.; Salernitano, E. *Carbon* **2006**, *44*, 671−674.
(12) Sonoyama, N.; Ohshita, M.; Nijubu, A.; Nishikawa, H.; Yanase, H.; Hayashi, J.-i.; Chiba, T. *Carbon* **2006**, *44*, 1754−1761.
(13) Sharma, S. P.; Lakkad, S. C. *Surf. Coat. Technol.* **2009**, *203*, 1329−1335.
(14) Kimiyoshi, N.; Jenn-Ming, Y.; Yoshihisa, T.; Yutaka, K. *Appl. Phys. Lett.* **2008**, *92*, 231912.
(15) Zhang, Q.; Liu, J.; Sager, R.; Dai, L.; Baur, J. *Compos. Sci. Technol.* **2009**, *69*, 594−601.
(16) J.J, B. *Mater. Sci. Eng.: A* **1990**, *126*, 203−223.
(17) Wicks, B. J. *J. Nucl. Mater.* **1975**, *56*, 287−296.
(18) Fitzer, E. *Carbon* **1989**, *27*, 621−645.
(19) Liu, J.; Tian, Y.; Chen, Y.; Liang, J.; Zhang, L.; Fong, H. *Mater. Chem. Phys.* **2010**, *122*, 548−555.
(20) Jawhari, T.; Roid, A.; Casado, J. *Carbon* **1995**, *33*, 1561−1565.
(21) Sadezky, A.; Muckenhuber, H.; Grothe, H.; Niessner, R.; Pöschl, U. *Carbon* **2005**, *43*, 1731−1742.
(22) Lee, S.; Kim, T.-R.; Ogale, A. A.; Kim, M.-S. *Synth. Met.* **2007**, *157*, 644−650.
(23) Liu, K.; Sun, Y.; Chen, L.; Feng, C.; Feng, X.; Jiang, K.; Zhao, Y.; Fan, S. *Nano Lett.* **2008**, *8*, 700−705.
(24) Nessim, G. D.; Hart, A. J.; Kim, J. S.; Acquaviva, D.; Oh, J.; Morgan, C. D.; Seita, M.; Leib, J. S.; Thompson, C. V. *Nano Lett.* **2008**, *8*, 3587−3593.
(25) Chhowalla, M.; Teo, K. B. K.; Ducati, C.; Rupesinghe, N. L.; Amaratunga, G. A. J.; Ferrari, A. C.; Roy, D.; Robertson, J.; Milne, W. I. *J. Appl. Phys.* **2001**, *90*, 5308−5317.
(26) Agnihotri, P.; Basu, S.; Kar, K. K. *Carbon* **2011**, *49*, 3098−3106.

(27) Montes-Mor, M. A.; Young, R. J. *Carbon* **2002**, *40*, 845−855.
(28) Huang, Y.; Young, R. J. *Carbon* **1995**, *33*, 97−107.
(29) Melanitis, N.; Tetlow, P. L.; Galiotis, C. *J. Mater. Sci.* **1996**, *31*, 851−860.
(30) Sinharoy, S.; Levenson, L. L. *Thin Solid Films* **1978**, *53*, 31−36.
(31) Hasebe, Y.; Kondoh, K.; Morita, K. *J. Nucl. Mater.* **1989**, *162*−*164*, 945−950.
(32) Chung, D. D. L. *Carbon Fiber Composites*; Butterworth-Heinemann: Boston, MA, 1994; p 215.
(33) Niwase, K. *Phys. Rev. B: Condens. Matter* **1995**, *52*, 15785−15798.
(34) Tang, Q.; Wu, J.; Sun, H.; Fang, S. *J. Alloys Compd.* **2009**, *475*, 429−433.